DOI: 10.1002/chem.200500038

Haloacyl Complexes of Boron, $[(CF_3)_3BC(O)Hal]^-$ (Hal = F, Cl, Br, I)

Maik Finze,*[a, b] Eduard Bernhardt,[a] Helge Willner,*[a] and Christian W. Lehmann[c]

Abstract: The haloacyltris(trifluoromethyl)borate anions $[(CF_3)_3BC(O)Hal]^-$ (Hal = F, Cl, Br, I) have been synthesized by reacting $(CF_3)_3BCO$ with either MHal (M = K, Cs; Hal = F) in SO_2 or MHal (M = $[nBu_4N]^+$, $[Et_4N]^+$, $[Ph_4P]^+$; Hal = Cl, Br, I) in dichloromethane. Metathesis reactions of the fluoroacyl complex with Me_3SiHal (Hal = Cl, Br, I) led to the formation of its higher homologues. The thermal stabilities of the haloacyltris(trifluoromethyl)borates decrease from the fluorine to the iodine derivative. The chemical reactivities decrease in the same order as demonstrated by a series of selected reactions. The new $[(CF_3)_3BC(O)Hal]^-$ (Hal = F, Cl, Br) salts are used as starting materials in the syntheses of novel compounds that contain the $(CF_3)_3B{-}C$ fragment. All borate anions $[(CF_3)_3BC(O)Hal]^-$ (Hal = F, Cl, Br, I) have been characterized by multinuclear NMR spectroscopy (^{11}B, ^{13}C, ^{17}O, ^{19}F) and vibrational spectroscopy. $[PPh_4][(CF_3)_3BC(O)Br]$ crystallizes in the monoclinic space group *P*2/*c* (no. 13) and the bond parameters are compared with those of $(CF_3)_3BCO$ and K-$[(CF_3)_3BC(O)F]$. The interpretation of the spectroscopic and structural data are supported by DFT calculations [B3LYP/6-311+G(d)].

Keywords: acyl halides · borates · density functional calculations · NMR spectroscopy · structure elucidation

Introduction

Since the discovery of the first tris(trifluoromethyl)boron derivative, $(CF_3)_3BNHEt_2$, 15 years ago,[1] numerous $(CF_3)_3B{-}N$ compounds have been prepared and transformed into other $(CF_3)_3B$ derivatives, for example $[(CF_3)_3BHal]^-$ (Hal = F, Cl, Br).[2,3] In contrast to $(CF_3)_3B{-}N$ derivatives, the chemistry of $(CF_3)_3B{-}C$ compounds has been little explored. In 2001 we reported the synthesis of the weakly coordinating tetrakis(trifluoromethyl)borate anion, $[B(CF_3)_4]^-$,[4] the first example of a $(CF_3)_3B{-}C$ species, by fluorination of the tetracyanoborate anion, $[B(CN)_4]^-$,[5,6] with ClF or ClF_3 in anhydrous HF.

It turns out that in concentrated sulfuric acid one of the CF_3 groups of $[B(CF_3)_4]^-$ is converted into a carbonyl ligand resulting in the unexpected borane carbonyl, $(CF_3)_3BCO$ [Eq. (1)].[7,8]

$$[B(CF_3)_4]^-_{(solv)} + H_3O^+ \xrightarrow[\text{conc. } H_2SO_4]{25\,^oC} (CF_3)_3BCO_{(g)} + 3HF_{(solv)} \quad (1)$$

This borane carbonyl is a main group analogue of homoleptic transition-metal-carbonyl cations[9–12] as exemplified by its high ν(CO) stretching frequency of 2267 cm^{-1} which is identical to the $\nu(CO)_{av}$ value of the superelectrophilic $[Ir(CO)_6]^{3+}$ cation.[13,14] Transition-metal-carbonyl cations are stabilized in fluoroantimonate salts which are extremely moisture sensitive, difficult to handle, and only soluble in superacids like aHF or aHF/SbF_5. Hence, their chemistry is limited to a few displacement reactions, for example, the displacement of CO by SO_3F^-, PF_3, and CH_3CN. Furthermore, only one example of an addition reaction at the CO ligand in $[Ir(CO)_6]^{3+}$, to yield $[Ir(CO)_5\{C(O)F\}]^{2+}$,[14] has been observed so far. In contrast to the salts of transition-metal-carbonyl cations, $(CF_3)_3BCO$ is a volatile compound,

[a] Dr. M. Finze, Dr. E. Bernhardt, Prof. Dr. H. Willner
FB C - Anorganische Chemie, Bergische Universität Wuppertal
Gaußstrasse 20, 42097 Wuppertal (Germany)
Fax: (+49) 202-439-3053
E-mail: maik.finze@uni-duesseldorf.de
willner@uni-wuppertal.de

[b] Dr. M. Finze
Present address: Institut für Anorganische Chemie und Strukturchemie II
Heinrich-Heine-Universität Düsseldorf
Universitätsstrasse 1, 40225 Düsseldorf (Germany)

[c] Dr. C. W. Lehmann
Max-Planck-Institut für Kohlenforschung
Kaiser-Wilhelm-Platz 1, 45470 Mülheim an der Ruhr (Germany)

Supporting information for this article is available on the WWW under http://www.chemeurj.org/ or from the author. A table of energies, enthalpies, and free energies of all compounds investigated by DFT calculations, a table of calculated thermodynamic data (DFT) for the reactions of $MeCO^+$ and FCO^+ with halide ions, tables of the calculated (DFT) and observed vibrations of $[(CF_3)_3BC(O)Hal]^-$ (Hal = F, Cl, Br, I) and tables of NMR isotopic shifts as well as relaxation rates.

easy to handle, and soluble in many organic solvents. It was found that $(CF_3)_3BCO$ reacts with nucleophiles either by addition to the electrophilic carbonyl carbon atom or in ligand-exchange reactions with the loss of CO.[8]

As previously outlined, $(CF_3)_3BCO$ is, on account of its spectroscopic and chemical properties, closely related to carbocations of the type RCO^+, for example, $MeCO^+$,[15] and to cationic transition-metal-carbonyl complexes.[8] Hence, the haloacyl complexes $[(CF_3)_3BC(O)Hal]^-$ (Hal = F, Cl, Br, I) are of special interest because they serve as links between acid halides in organic chemistry and haloacyl complexes in transition-metal chemistry.

The synthesis as well as the spectroscopic and structural properties of the first fluoroacyl complex of boron, $[(CF_3)_3BC(O)F]^-$, have been presented in a short communication.[16] It was obtained in SO_2 solution according to Equation (2).

$$(CF_3)_3BCO + MF \xrightarrow{SO_{2(l)}} M[CF_3)_3BC(O)F] \quad (M = K, Cs) \tag{2}$$

As an extension to the work described in this communication we herein report on 1) the syntheses of further haloacyl complexes $[(CF_3)_3BC(O)Hal]^-$ (Hal = Cl, Br, I), 2) the thermal stabilities of the $[(CF_3)_3BC(O)Hal]^-$ (Hal = F, Cl, Br, I) complexes in different salts using differential scanning calorimetry (DSC), 3) the reactions of the haloacylborate anions with selected nucleophiles, 4) a complete characterization of the borate anions by heteronuclear NMR and vibrational spectroscopy, 5) the structure of $[PPh_4][(CF_3)_3BC(O)Br]$ determined by single-crystal X-ray diffraction, and 6) DFT calculations, which support the vibrational assignments and interpretation of the bonding parameters.

In contrast to $(CF_3)_3BCO$, salts of the haloacyl complexes are thermally stable and are the key starting materials for a diverse chemistry. $[B(CF_3)_4]^-$ and related anions, for example, $[(CF_3)_3BCPnic]^-$ (Pnic = N, P, As)[17,18] and $[(CF_3)_3BNC]^-$,[18] exhibit unusual properties enabling their application in many fields of growing interest, such as ionic liquids, catalysts, electrolytes, and weakly coordinating anions. Therefore the syntheses of new derivatives that contain the $(CF_3)_3B$ group are of general interest.

Results and Discussion

Syntheses of M[$(CF_3)_3BC(O)F$] (M = K, Cs)—reactions of alkali metal halides with $(CF_3)_3BCO$ in liquid SO_2: In the syntheses [Eq. (2)] of alkali metal salts that incorporate the $[(CF_3)_3BC(O)F]^-$ ion, the reaction time is of importance[16] because prolonged reaction times result in decreased yields and the formation of the diborate anion $[\{(CF_3)_3BC(O)\}_2O]^{2-}$. This can be rationalized by nucleophilic attack by SO_2F^-[19] on the carbon atom of the acyl group of $[(CF_3)_3BC(O)F]^-$ resulting in $[(CF_3)_3BCO_2]^{2-}$ followed by reaction with a second equivalent of $[(CF_3)_3BC(O)F]^-$ [Eqs. (3) and (4)].

$$[(CF_3)_3BC(O)F]^- + SO_2F^- \rightarrow [(CF_3)_3BCO_2]^{2-} + SOF_2 \tag{3}$$

$$[(CF_3)_3BCO_2]^{2-} + [(CF_3)_3BC(O)F]^- \rightarrow [\{(CF_3)_3BC(O)\}_2O]^{2-} + F^- \tag{4}$$

In contrast to the syntheses of $[(CF_3)_3BC(O)F]^-$ salts, treatment of $(CF_3)_3BCO$ with alkali metal chlorides, bromides, or iodides in liquid sulfur dioxide resulted in complex product mixtures without the formation of the desired haloacylborate anions, $[(CF_3)_3BC(O)Hal]^-$ (Hal = Cl, Br, I). Some of the isolated products were identified as $[(CF_3)_3BC(O)OH]^-$ and $[\{(CF_3)_3BC(O)\}_2O]^{2-}$ salts. It is assumed that a similar degradation process to that described by Equations (3) and (4) occurs with the halosulfinate anions formed in these systems.[19,20] The different behavior of $[(CF_3)_3BC(O)F]^-$ in comparison to its higher homologues is probably due to its lower reactivity. Increasing reactivities of isovalent-electronic haloacyl derivatives from fluoro to iodo derivatives ($F < Cl < Br \ll I$) are well known in organic chemistry.[21]

Syntheses of M[$(CF_3)_3BC(O)Hal]^-$ (M=[$nBu_4N]^+$, [$Et_4N]^+$, [$Ph_4P]^+$; Hal = Cl, Br, I) from $(CF_3)_3BCO$: The other haloacylborate anions $[(CF_3)_3BC(O)Hal]^-$ (Hal = Cl, Br, I) were obtained by the reactions of halide salts containing weakly coordinating cations with $(CF_3)_3BCO$ in dichloromethane solution according to Equation (5).

$$(CF_3)_3BCO + MHal \xrightarrow{CH_2Cl_2} M[(CF_3)_3BC(O)Hal] \tag{5}$$

($M = [nBu_4N]^+$, Hal = Cl, Br, I; $M = [Et_4N]^+$, Hal = Cl; $M = [Ph_4P]^+$ Hal = Cl, Br)

The $[(CF_3)_3BC(O)Hal]^-$ (Hal = Cl, Br, I) salts were isolated as colorless solids by removing the solvent. Impurities (~2%) such as the $[(CF_3)_3BC(O)OH]^-$ anion were due either to the presence of $(CF_3)_3BC(OH)_2$[8] in the starting material or to traces of water in the reaction mixtures.

To complete the series of $[nBu_4N]^+$ salts in Equation (5), the fluoroacylborate derivative was synthesized by a metathesis reaction [Eq. (6)].

$$K[(CF_3)_3BC(O)F] + [nBu_4N]Cl \xrightarrow{CH_2Cl_2} [nBu_4N][(CF_3)_3BC(O)F] + KCl\downarrow \tag{6}$$

The $[(CF_3)_3BC(O)Hal]^-$ (Hal = F, Cl, Br) anions are stable at room temperature in acetonitrile solution but the corresponding iodo derivative slowly decomposes into $(CF_3)_3BNCMe$,[8,22] CO, and I^-.

The $[(CF_3)_3BC(O)Hal]^-$ anions are the first examples of mononuclear boron haloacyl derivatives. Early attempts to synthesize a chloroacyl complex of H_3BCO by addition of chloride failed and instead yielded $(MeBO)_3$.[23] A few examples of boron clusters that contain the chloroacyl substituent, for example, 9-chloroacyl-1,2-dicarba-*closo*-dodecaborane, have been described[24,25] and their chemistry has been studied to some extent.[24,26] As discussed above

$(CF_3)_3BCO$ is a main group analogue of homoleptic transition-metal-carbonyl cations,[9–12] but only one example of the formation of a haloacyl complex from a homoleptic transition-metal-carbonyl cation, $[Ir(CO)_6]^{3+}$, is known: $[Ir(CO)_5\{C(O)F\}]^{2+}$.[14] There are only a limited number of reports on related transition-metal complexes: $[Ir(CO)_2F\{C(O)F\}(PEt_3)]^+$,[27] $[MF\{C(O)F\}(CO)_2(PPh_3)_2]$ (M = Ru, Os),[28] and $[CpRe(CO)_2Br\{C(O)Br\}]$.[29]

To study the effect of the cation on the stability of the $[(CF_3)_3BC(O)Cl]^-$ ion, attempts were made to prepare the corresponding $[Et_3NH]^+$, $[H(OEt_2)_2]^+$, and NO^+ salts. The main product of the reaction between $[Et_3NH]Cl$ and $(CF_3)_3BCO$ in CD_2Cl_2 was $[Et_3NH][(CF_3)_3BC(O)Cl]_{(solv)}$ with the anions $[(CF_3)_3BCl]^-$,[30] $[(CF_3)_3BF]^-$,[30,31] and other perfluoroalkylfluoroborates[31] formed as impurities. At room temperature $[Et_3NH][(CF_3)_3BC(O)Cl]$ slowly decomposed into $[Et_3NH][(CF_3)_3BCl]$ and CO.

HCl reacts with $(CF_3)_3BCO$ in diethyl ether solution to give the insoluble $[H(OEt_2)_2][(CF_3)_3BC(O)Cl]$ [Eq. (7)].

$$(CF_3)_3BCO + HCl + 2Et_2O \xrightarrow{Et_2O} [H(OEt_2)_2][(CF_3)_3BC(O)Cl]_{(s)} \quad (7)$$

This salt was isolated at −30 °C by removal of excess diethyl ether under reduced pressure. The formation of the $[H(OEt_2)_2]^+$ cation was proved by its ^1H NMR spectrum in CD_2Cl_2 which shows the characteristic signal of the bridging acidic proton at $\delta = 16.3$ ppm and the signals of the ether protons shifted to higher frequencies relative to those of neat Et_2O (compare with, for example, $[H(OEt_2)_2][B(C_6F_5)_4]$[32]). At room temperature under vacuum reaction (7) is reversible. Under nitrogen $[H(OEt_2)_2][(CF_3)_3BC(O)Cl]$ slowly decomposes into HCl, Et_2O, and a series of other borate anions containing the $(CF_3)_3B{-}C$ fragment as well as traces of $[(CF_3)_3BCl]^-$[30] and $[(CF_3)_3BF]^-$.[30,31]

Nitrosyl chloride undergoes a ligand-exchange reaction with $(CF_3)_3BCO$ to give $NO[(CF_3)_3BCl]$ as the main product [Eq. (8)].

$$(CF_3)_3BCO + NOCl \rightarrow NO[(CF_3)_3BCl] + CO \quad (8)$$

In summary, the $[(CF_3)_3BC(O)Cl]^-$ ion is only stable at room temperature in salts with weakly coordinating cations.

Reactions with Me_3SiHal (Hal = Cl, Br, I): The reactions of $[(CF_3)_3BC(O)F]^-$ with Me_3SiHal (Hal = Cl, Br, I) in dichloromethane or acetonitrile solution according to Equation (9) provide an alternative synthetic approach towards $[(CF_3)_3BC(O)Hal]^-$ (Hal = Cl, Br, I).

$$[(CF_3)_3BC(O)F]^- + Me_3SiHal \rightarrow [(CF_3)_3BC(O)Hal]^- + Me_3SiF \quad (9)$$

(Hal = Cl, Br, I)

The bromo- and iodoacyl derivatives are also accessible from $[(CF_3)_3BC(O)Cl]^-$ and the corresponding trimethylsilyl halides. If the potassium salt of $[(CF_3)_3BC(O)F]^-$ is used as the starting material [Eq. (9)], $[(CF_3)_3BC(O)Hal]^-$ is initially observed by NMR spectroscopy, but subsequently KHal precipitates and CO as well as $(CF_3)_3BNCMe$ are formed in acetonitrile solution. The intermediate $(CF_3)_3BCO$ cannot be detected as a result of its fast reaction with acetonitrile [Eq. (10)].[8]

$$K[(CF_3)_3BC(O)F] \xrightarrow[-Me_3SiF]{+Me_3SiHal} K[(CF_3)_3BC(O)Hal] \xrightarrow[-KHal]{} (CF_3)_3BCO \xrightarrow[-CO]{+MeCN} (CF_3)_3BNCMe \quad (10)$$

(Hal = Cl, Br, I)

The decomposition rate of $[(CF_3)_3BC(O)Hal]^-$ monitored qualitatively by NMR spectroscopy increases in the order: $[(CF_3)_3BC(O)Cl]^- < [(CF_3)_3BC(O)Br]^- < [(CF_3)_3BC(O)I]^-$. This observation parallels the reactivities of the haloacylborate anions discussed in previous sections.

A few examples of transformations of acid chlorides into acid iodides employing Me_3SiI are known in organic chemistry.[33,34]

Chemical properties of $[(CF_3)_3BC(O)Hal]^-$ (Hal=F, Cl, Br, I)—an overview: The straightforward, high-yield, and easily scaled-up syntheses of salts containing the haloacylborate anions $[(CF_3)_3BC(O)Hal]^-$ (Hal = F, Cl, Br, I) enable the preparation of new $(CF_3)_3B{-}C$ compounds. The reactions of $[(CF_3)_3BC(O)F]^-$ and $[(CF_3)_3BC(O)Cl]^-$ with selected nucleophiles, which have been investigated so far, are summarized in Scheme 1. They have either been published {$[(CF_3)_3BCPnic]^-$ (Pnic = N, P, As),[17,18] $[(CF_3)_3BC(O)NR^1R^2]^-$ (R^1 = H, Me; R^2 = H, Me, *n*Pr)[35]}, are included in the Experimental Section (reactions with Me_3SiHal), or will be published elsewhere in detail {$[(CF_3)_3BC(O)CN]^-$, $[(CF_3)_3BC(OSiMe_3)(CN)_2]^-$}. The chemistry of the bromoacyl derivative is similar to that of its chloro analogue while $[(CF_3)_3BC(O)I]^-$ is too reactive and hence it is not a suitable reagent for the synthesis of $(CF_3)_3B{-}C$ derivatives.

While most of the reactions of the haloacylborate anions are similar to the reactions of their parent compound $(CF_3)_3BCO$, for example, the synthesis of the $[(CF_3)_3BCN]^-$ ion using $K[N(SiMe_3)_2]$[8] or the formation of $[(CF_3)_3BC(O)OH]^-$ by the reaction with water,[8] there are some important differences. Most significantly, in the reactions of $K[Pnic(SiMe_3)_2]$ (Pnic = P, As) with $[(CF_3)_3BC(O)Hal]^-$ (Hal = Cl, Br) the highly unusual borates $[(CF_3)_3BCPnic]^-$ (Hal = P, As)[17] are obtained, while with $[(CF_3)_3BC(O)F]^-$ the dianions $[(CF_3)_3BC(OSiMe_3)PnicC(O)B(CF_3)_3]^{2-}$ are formed. The corresponding reaction with $(CF_3)_3BCO$ results in a complex product mixture. The formation of different products is due to a decrease in reactivity in the order $(CF_3)_3BCO > [(CF_3)_3BC(O)I]^- > [(CF_3)_3BC(O)Br]^- \sim [(CF_3)_3BC(O)Cl]^- > [(CF_3)_3BC(O)F]^-$.

As starting materials for the syntheses of novel borate anions containing the $(CF_3)_3B{-}C$ fragment, the

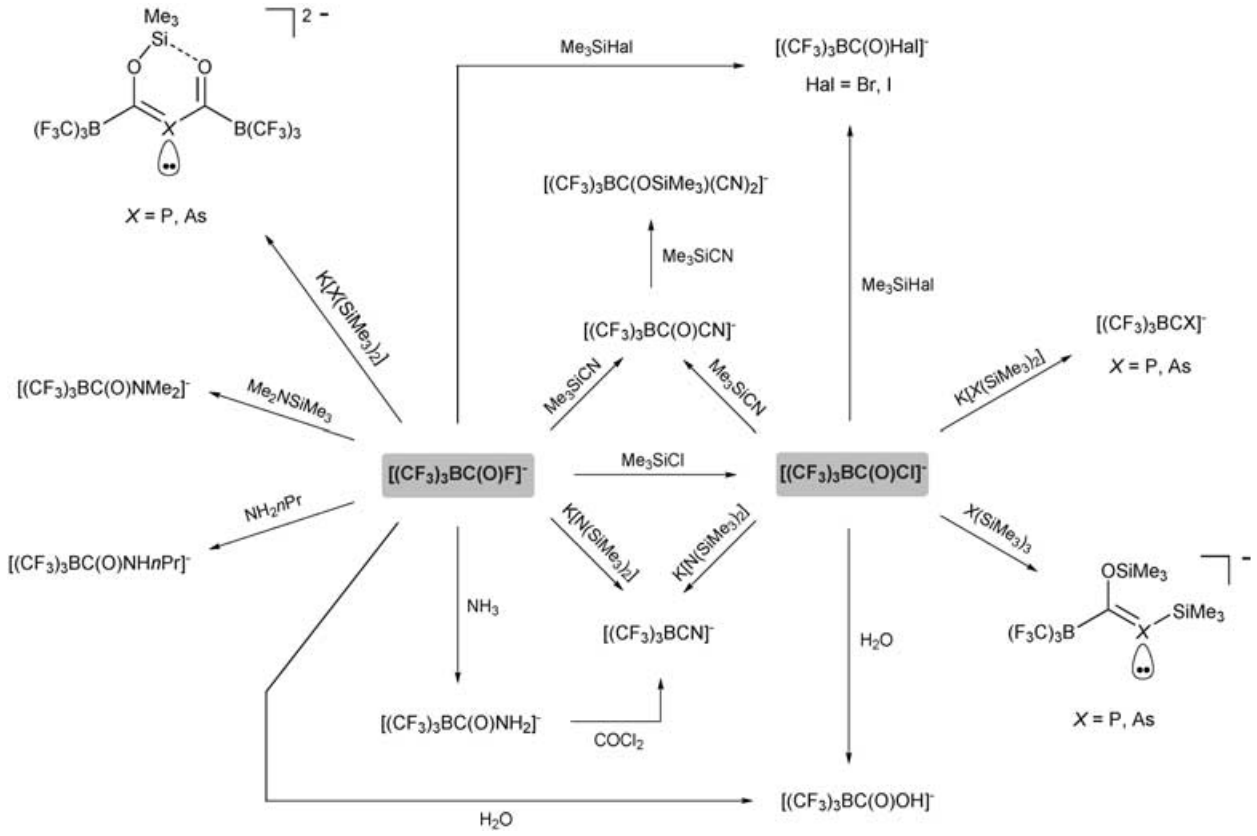

Scheme 1. Selected reactions of $[(CF_3)_3BC(O)F]^-$ and $[(CF_3)_3BC(O)Cl]^-$.

$[(CF_3)_3BC(O)Hal]^-$ (Hal = F, Cl, Br) anions have some advantages over the parent compound $(CF_3)_3BCO$: 1) they are thermally stable solids that can be handled under an inert atmosphere without using vacuum techniques and 2) owing to their enhanced stability, reactions can be performed in coordinating solvents that react with the borane carbonyl, for example, THF or acetonitrile.[8]

Thermal properties: The thermal stabilities of $[n\mathrm{Bu}_4\mathrm{N}][(CF_3)_3BC(O)Hal]$ (Hal = F, Cl, Br, I) have been investigated by differential scanning calorimetry (DSC) and the results are summarized in Table 1. In these tetrabutylammonium salts the thermal stabilities decrease with increasing atomic number of the halogen atom. This trend is in agreement with the reactivities and the behavior of organic acid halides discussed above. The decomposition products obtained from the DSC experiments were analyzed by NMR spectroscopy and in all cases the main products were the borate anions $[C_2F_5BF_3]^-$[31] and $[(CF_3)_3BF]^-$.[30,31] The formation of $[C_2F_5BF_3]^-$ can be explained by an intramolecular rearrangement reaction similar to the degradation of $(CF_3)_3BCO$ in the gas phase or in anhydrous HF.[31] The formation of $[(CF_3)_3BF]^-$ during the decomposition of $[(CF_3)_3BC(O)Hal]^-$ (Hal = Cl, Br, I) can be rationalized by an intermolecular fluoride ion transfer from a CF_3 group. The borate anions $[(CF_3)_3BCl]^-$ and $[(CF_3)_3BBr]^-$ have also been identified in the reaction mixtures obtained from DSC experiments on $[n\mathrm{Bu}_4\mathrm{N}][(CF_3)_3BC(O)Cl]$ and $[n\mathrm{Bu}_4\mathrm{N}][(CF_3)_3BC(O)Br]$.[30] The so far unknown $[(CF_3)_3BI]^-$ ion might also be formed during the decomposition of the iodoacylborate anion but owing to the formation of many compounds, an assignment of the NMR signals was not possible.

Table 1. Thermal data of salts of the $[(CF_3)_3BC(O)Hal]^-$ (Hal = F, Cl, Br, I) anions, determined by DSC measurements.

Compound	$T_{\text{phase transition}}$ [°C]	$T_{\text{melting point}}$ [°C]	$T_{\text{decomposition}}$ [°C]
$K[(CF_3)_3BC(O)F]$	−41		130
$Cs[(CF_3)_3BC(O)F]$	67		140
$[n\mathrm{Bu}_4\mathrm{N}][(CF_3)_3BC(O)F]$		145	180
$[n\mathrm{Bu}_4\mathrm{N}][(CF_3)_3BC(O)Cl]$		133	166
$[\mathrm{Et}_4\mathrm{N}][(CF_3)_3BC(O)Cl]$			145
$[\mathrm{Ph}_4\mathrm{P}][(CF_3)_3BC(O)Cl]$		183[a]	183[a]
$[n\mathrm{Bu}_4\mathrm{N}][(CF_3)_3BC(O)Br]$		100[a]	100[a]
$[\mathrm{Ph}_4\mathrm{P}][(CF_3)_3BC(O)Br]$			
$[n\mathrm{Bu}_4\mathrm{N}][(CF_3)_3BC(O)I]$		60[a,b]	60[a,b]

[a] Decomposes during melting. [b] Slow decomposition at room temperature.

The thermal stabilities of different salts of the $[(CF_3)_3BC(O)F]^-$ ion nicely demonstrate the effect of the cation. The fluoroacylborate salt becomes more stable (Table 1) as the size of the cation increases ($K^+ < Cs^+ < [n\mathrm{Bu}_4\mathrm{N}]^+$). The stability of $[n\mathrm{Bu}_4\mathrm{N}][(CF_3)_3BC(O)F]$ is un-

precedented, being stable up to 180 °C as a molten salt (T_{mp} = 145 °C).

Quantum-chemical calculations: The reactions of halide ions with $(CF_3)_3BCO$ were studied by DFT calculations at the B3LYP/6-311++G(d) level of theory and the thermochemical data are summarized in Table 2 (all energies and free energies are collected in Table S1 in the Supporting Information). Two different types of reactions were considered: 1) the addition of the halide ion to the carbon atom of the carbonyl ligand of $(CF_3)_3BCO$ and 2) the ligand exchange reaction that yields $[(CF_3)_3BHal]^-$ (Hal = F, Cl, Br, I) and carbon monoxide. The data obtained demonstrate that the formation of $[(CF_3)_3BC(O)Hal]^-$ (Hal = F, Cl, Br, I) is kinetically controlled, since the ligand-exchange reaction is thermodynamically favored. The decrease in the enthalpy of formation from $[(CF_3)_3BC(O)F]^-$ to $[(CF_3)_3BC(O)I]^-$ is in agreement with the decreasing thermal stability as discussed in the previous section and the increasing reactivity of these anions. The enthalpies also parallel the general experimental observations in C–Hal dissociation energies[36] and a similar trend in the calculated reaction enthalpies is also found for the two related series MeC(O)Hal and FC(O)Hal (Hal = F, Cl, Br, I) (see Table S2 in the Supporting Information).

Table 2. Calculated[a] thermodynamic data for the reactions of $(CF_3)_3BCO$ with halides yielding either $[(CF_3)_3BC(O)Hal]^-$ or $[(CF_3)_3BHal]^-$ (Hal = F, Cl, Br, I).

Hal^-	ΔH [kJ mol^{-1}]	ΔG [kJ mol^{-1}]
	$(CF_3)_3BCO + Hal^- \rightarrow$	$[(CF_3)_3BC(O)Hal]^-$
F^-	−384.8	−350.9
Cl^-	−207.8	−175.0
Br^-	−175.5	−144.6
I^-	−140.6	−108.5
	$(CF_3)_3BCO + Hal^- \rightarrow [(CF_3)_3BHal]^- + CO$	
F^-	−432.1	−439.2
Cl^-	−248.0	−248.4
Br^-	−201.7	−211.4
I^-	−153.9	−161.4

[a] At the B3LYP/6-311+G(d) level of theory (SDD for iodine).

The crystal structure of $[Ph_4P][(CF_3)_3BC(O)Br]$: The solid-state structure of $[Ph_4P][(CF_3)_3BC(O)Br]$ was obtained by single-crystal X-ray diffraction. The experimental details and crystal data are summarized in Table 3. Table 4 allows selected bond parameters of the anion to be compared with those of the $[(CF_3)_3BC(O)F]^-$ ion in the K^+ salt,[16] with those of $(CF_3)_3BCO$ in the gas phase as well as in the solid state,[8] and with values obtained from DFT calculations on $(CF_3)_3BCO$ and $[(CF_3)_3BC(O)Hal]^-$ (Hal = F, Cl, Br, I). The structure of the bromoacylborate anion in $[Ph_4P][(CF_3)_3BC(O)Br]$ is shown in Figure 1.

In the solid-state structure of $[Ph_4P][(CF_3)_3BC(O)Br]$ the anions and cations form staples along the *b* axes (see Figure S1 in the Supporting Information). The closest distances between anions and cations are in the range of weak interionic contacts.[37] In the crystal the anions exhibit C_1 local symmetry but the deviation from C_s symmetry is very small as the bromoacyl substituent is rotated from the mirror plane by only 7.5° (Figure 1). From the calculated structure of the borate anion at the energy minimum [B3LYP/6-311+G(d)] it can be predicted that there should be an even smaller deviation from C_s symmetry with a torsion angle of 0.4° and with an energy difference between C_1 and C_s symmetry of less than 1 kJ mol^{-1}. All other differences between the measured (solid state) and calculated (gas phase) bond parameters of the $[(CF_3)_3BC(O)Br]^-$ anion are small (Table 4) and are of the same order as found previously for $[(CF_3)_3BC(O)F]^-$.[16] In agreement with the orientation of the C(O)F ligand in the fluoroacylborate complex in which the fluorine atom points into the gap between two of the three CF_3 groups,[16] the bromine atom protrudes between two trifluoromethyl substituents and the oxygen atom is adjacent to the third CF_3 ligand (Figure 1).

Table 3. Crystallographic data for $[Ph_4P][(CF_3)_3BC(O)Br]$.[a]

chemical formula	$C_{28}H_{20}BBrF_9OP$
formula weight [g mol^{-1}]	665.13
temperature [K]	100
color	colorless
crystal size [mm^3]	0.44 × 0.10 × 0.08
crystal system, space group	monoclinic, *P*2/*c* (no. 13)
a [Å]	18.5200(3)
b [Å]	7.5999(1)
c [Å]	19.3649(3)
β [°]	91.182(1)
volume [Å^3]	2725.03(7)
Z	4
ρ_{calcd} [Mg m^{-3}]	1.621
absorption coefficient [mm^{-1}]	1.651
F(000) [e]	1328
θ range [°]	3.41–31.05
index range	$-26 \le h \le 26$, $-10 \le k \le 11$, $-28 \le l \le 28$
reflections collected/unique	35092/8646
reflections observed [$I > 2\sigma(I)$]	6623
R(int) [%]	6.16
data/restraints/var. par.	8646/0/371
R_1 [$I > 2\sigma(I)$][b] [%]	5.60
R_1 (all)[b] [%]	8.01
wR_2 [$I > 2\sigma(I)$][c] [%]	16.89
wR_2 (all)[c] [%]	14.81
goodness-of-fit on F^2[d]	1.043
largest diff. peak/hole [e Å^{-3}]	0.875/−0.920

[a] CCDC 252158 contains the supplementary crystallographic data for this paper. These data can be obtained free of charge from the Cambridge Crystallographic Data Centre via www.ccdc.cam.ac.uk/data_request/cif. [b] $R_1 = (\Sigma \| F_o | - | F_c \|) / \Sigma | F_o |$. [c] $R_w = [\Sigma w(F_o^2 - F_c^2)^2 / \Sigma w F_o^2]^{1/2}$, weight scheme: $w = [\sigma^2 F_o + (0.0871P)^2 + 4.1956P]^{-1}$; $P = [\max(0, F_o^2) + 2F_c^2]/3$. [d] Goodness-of-fit $S = \Sigma w(F_o^2 - F_c^2)^2/(m-n)$; ($m$ = reflections, n = variables).

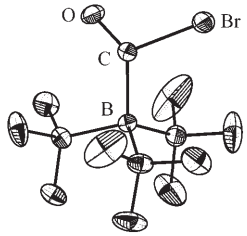

Figure 1. Structure of the $[(CF_3)_3BC(O)Br]^-$ ion in $[Ph_4P][(CF_3)_3BC(O)Br]$ (50% probability ellipsoids).

Models of the optimized structures of the haloacylborate anions $[(CF_3)_3BC(O)Hal]^-$ as

Table 4. Experimental[a] and calculated[b] bond parameters of $[(CF_3)_3BC(O)Hal]^-$ (Hal = F, Cl, Br, I).

	$[(CF_3)_3BC(O)F]^-$[c]		$[(CF_3)_3BC(O)Cl]^-$	$[(CF_3)_3BC(O)Br]^-$		$[(CF_3)_3BC(O)I]^-$	$(CF_3)_3BCO$[d]		
	solid	calcd	calcd	solid	calcd	calcd	solid	gas phase	calcd
symmetry	C_1	C_s	C_s	C_1	C_s	C_s	C_1	C_3	C_3
bond lengths									
C–O	1.208(4)	1.186	1.176	1.167(4)	1.170	1.165	1.11(2)	1.124	1.119
C(O)–Hal	1.351(4)	1.406	1.933	2.064(3)	2.147	2.448	–	–	–
B–C(O)Hal	1.621(5)	1.635	1.647	1.634(4)	1.652	1.657	1.69(2)	1.617(12)	1.589
B–CF_3	1.622(5)	1.646	1.648	1.623(4)	1.648	1.647	1.60(2)	1.631(4)	1.646
C–F	1.387(3)	1.368	1.366	1.340(4)	1.366	1.365	1.35(2)	1.348(1)	1.354
bond angles									
B–C–O	126.8(3)	131.5	130.2	131.25(26)	130.7	131.0	177.1(15)	180.0	180.0
B–C(O)–Hal	112.8(3)	112.0	114.9	113.97(18)	115.5	117.0	–	–	–
O–C–Hal	120.5(3)	116.5	115.0	114.70(21)	113.8	112.0	–	–	–
B–C(O)Hal	109.5(2)	108.9	108.8	108.9(2)	108.6	108.3	104.4(12)	103.8(4)	105.5
C–B–C	109.4(2)	110.1	110.1	110.0(2)	110.3	110.5	114.0(12)	114.5(4)	113.1
F–C–F	104.5(2)	105.1	105.2	104.9(2)	105.3	105.4	107.2(1)	107.2(1)	106.9
torsion angle									
F_3C–B–C(O)–Hal	180.0(2)	171.5	177.4	173.5(2)	179.6	180	–	–	–

[a] For different bond lengths and angles mean values are calculated. [b] At the B3LYP/6-311+G(d) level of theory (SDD for iodine). [c] See reference [16]. [d] See reference [8].

well as those of the related compounds MeC(O)Hal and FC(O)Hal (Hal = F, Cl, Br, I) are depicted in Figure 2 and selected bond parameters are also presented. The calculated values are in good agreement with the experimental bond lengths and angles. There are several important differences between the three series of compounds: 1) *d*(C(O)–Hal) values decrease from the borate anions to *d*(MeC(O)–Hal) and *d*(FC(O)–Hal) and 2) $[(CF_3)_3BC(O)Hal]^-$ exhibits the smallest O–C–Hal angles and FC(O)Hal the largest. Both trends can be attributed to the large steric demand of the $(CF_3)_3B$ group relative to that of the fluorine atom and the methyl group as well as to the different charges—the boron derivatives are anions while the members of the other two series are neutral molecules. The steady changes from fluorine to iodine for the three related series is due to a stronger interaction with the other substituent, $(CF_3)_3B$, Me or F, bound to the carbonyl group.

Within the RC(O)Hal series, the *d*(C–O) value decreases with increasing mass of the halogen atom, except for the COF_2/FC(O)Cl couple for which identical bond lengths were calculated.

NMR spectra: Except for the NMR-active nuclei of chlorine, bromine, iodine, and ^{10}B, all the nuclei in the haloacylborate anions $[(CF_3)_3BC(O)Hal]^-$ (Hal = F, Cl, Br, I) that exhibit a spin of $S = 0$ were investigated by NMR spectroscopy (^{11}B, ^{13}C, ^{17}O, ^{19}F). The chemical shifts and coupling constants are summarized in Table 5 and the isotopic shifts[50] are collected in Table S7 in the Supporting Information. The chemical shifts are similar to those of related compounds that contain the $(CF_3)_3B$–C fragment[4,8,17,18] and to a lesser extent to other $(CF_3)_3B$–*X* compounds.[2,3] The NMR spectroscopic data for $(CF_3)_3BCO$[8] and $[B(CF_3)_4]^-$[4] are included in Table 5 and Table S7 in the Supporting Information for comparison.

The ^{11}B NMR spectra of $[(CF_3)_3BC(O)Hal]^-$ (Hal = F, Cl, Br, I) and of $(CF_3)_3BCO$ are depicted in Figure 3. The ^{11}B chemical shifts are comparable to the values of related compounds, for example, $[B(CF_3)_4]^-$[4] and $[(CF_3)_3BC(O)OH]^-$.[8] $[(CF_3)_3BC(O)Br]^-$ is found to have the highest $\delta(^{11}B)$ value in the series. All ^{11}B NMR signals are split into decets as a result of coupling with the nine equivalent ^{19}F nuclei of the CF_3 groups. The $^2J(^{11}B,^{19}F)$ coupling constants of $[(CF_3)_3BC(O)Hal]^-$ (Hal = F, Cl, Br, I) are approximately 27 Hz (Table 5). These coupling constants are larger than that of $[B(CF_3)_4]^-$ [$^2J(^{11}B,^{19}F) = 25.9$ Hz][4] and smaller than that of the parent borane carbonyl [$^2J(^{11}B,^{19}F) = 36 \pm 2$ Hz],[8] indicating weaker B–CF_3 bonds in $[B(CF_3)_4]^-$ and stronger B–CF_3 bonds in $(CF_3)_3BCO$. In addition to the interaction with the nine ^{19}F nuclei of the CF_3 groups the ^{11}B nucleus of $[(CF_3)_3BC(O)F]^-$ couples to the ^{19}F nucleus of the fluoroacyl ligand (Figure 3).[16]

The increase in the line widths of the ^{11}B NMR signals in the order $[(CF_3)_3BC(O)F]^- < [(CF_3)_3BC(O)Cl]^- < [(CF_3)_3BC(O)Br]^- < [(CF_3)_3BC(O)I]^- < (CF_3)_3BCO$ (Figure 3, Table S8 in the Supporting Information) reflects the C(O)–Hal bond strengths (Table 2): F^- forms the strongest bond with the carbon atom of the carbonyl ligand, the C(O)–I bond is the weakest in the isovalent-electronic series, and in $(CF_3)_3BCO$ no substituent is attached to the CO ligand. Broad signals are typical for ^{11}B NMR spectroscopy and are due to the electric-field gradient at the quadrupolar ^{11}B nucleus.[51–53] In Table S8 in the Supporting Information, the measured T_1 values for $[(CF_3)_3BC(O)Hal]^-$ (Hal = F, Cl, Br, I), $(CF_3)_3BCO$,[8] and $[B(CF_3)_4]^-$[8] are compared with the corresponding T_2 values which have been calculated from the observed line widths.

The resonances of the CF_3 groups in the ^{19}F NMR spectra of $[(CF_3)_3BC(O)Hal]^-$ (Hal = F, Cl, Br, I) and $(CF_3)_3BCO$ are presented in Figure 4. The ^{19}F resonance frequency increases from the fluoroacyl derivative to the borane carbonyl. Owing to the coupling with ^{11}B, the signals are split into quartets and in the case of $[(CF_3)_3BC(O)F]^-$ the signal is further split into a doublet as a result of $^4J(C^{19}F_3,C(O)^{19}F)$

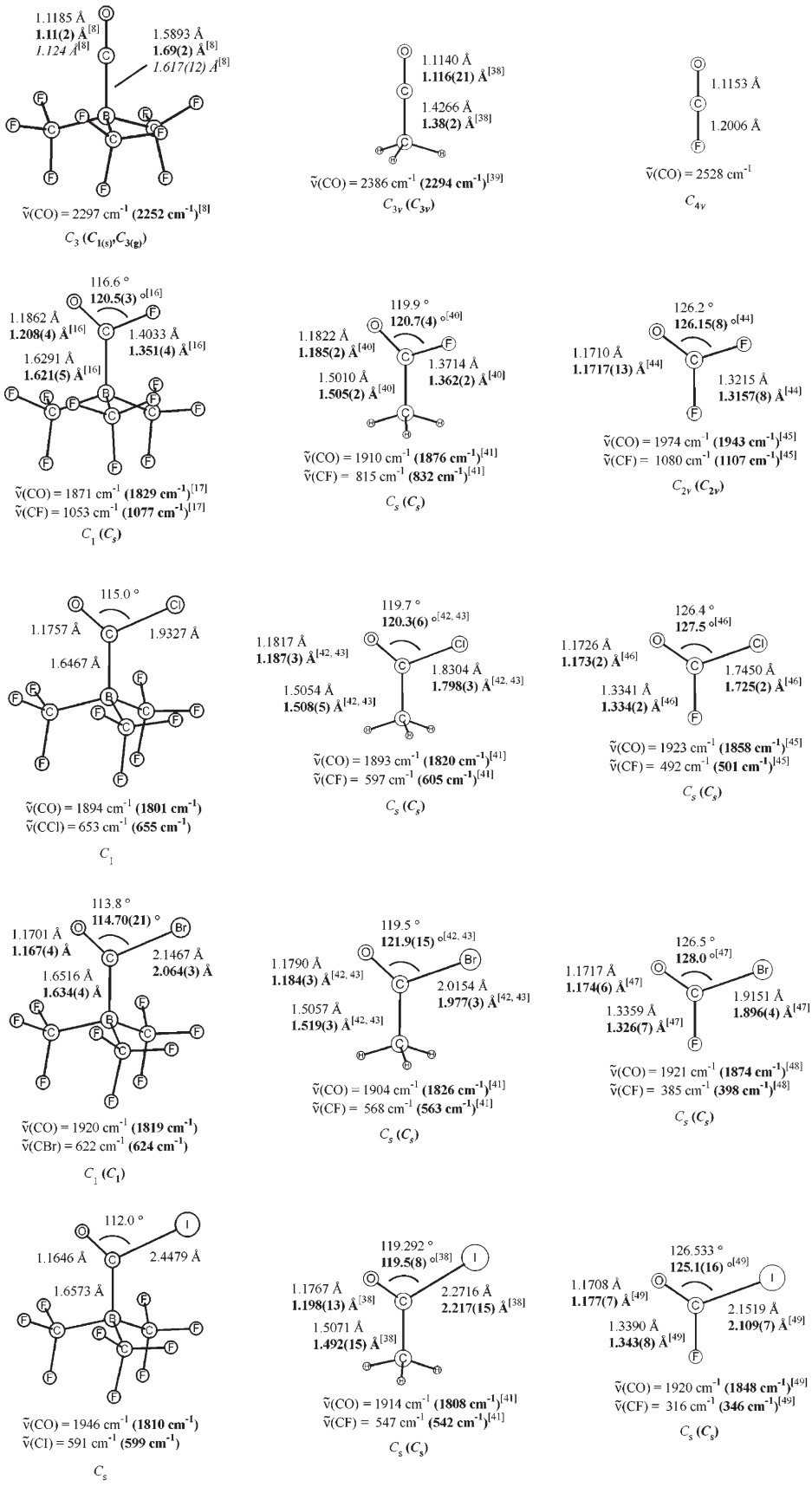

Figure 2. Calculated structures (bold typeface) and experimental bond parameters (normal typeface) for $(CF_3)_3BCO$, $MeCO^+$, FCO^+, $[(CF_3)_3BC(O)Hal]^-$, MeC(O)Hal, and FC(O)Hal (Hal = F, Cl, Br, I).

Table 5. NMR spectroscopic data for $[(CF_3)_3BC(O)Hal]^-$ (Hal = F, Cl, Br, I), $(CF_3)_3BCO$, and $[B(CF_3)_4]^-$.[a,b]

Parameter	$[(CF_3)_3BC(O)F]^-$	$[(CF_3)_3BC(O)Cl]^-$	$[(CF_3)_3BC(O)Br]^-$	$[(CF_3)_3BC(O)I]^-$	$(CF_3)_3BCO$[c]	$[B(CF_3)_4]^-$
$\delta(^{11}B)$	−19.1	−16.0	−15.2	−15.4	−17.9	−18.9
$\delta(^{13}C)$ (CF_3)	132.8	132.3	131.5	130.1[c]	126.2	132.9
$\delta(^{13}C)$ (CO)	173.7	186.5	185.8	188.9[c]	159.8	
$\delta(^{17}O)$	412	549	570	612[c]	342	
$\delta(^{19}F)$ (CF_3)	−61.2	−60.4	−60.2	−59.8	−58.7	−61.6
$\delta(^{19}F)$ (C(O)F)	78.3					
$^1J(^{11}B,^{13}CF_3)$	74.6	75.8	76.8	76.7	80 ± 5	73.4
$^1J(^{11}B,^{13}CO)$	73.1	70.3	67.5	60.9	30 ± 5	
$^1J(^{13}CF_3,C^{19}F_3)$	303.9	304.3	303.9	304.6	298.9	304.3
$^1J(^{13}CF_3,C(O)^{19}F)$	398.0					
$^2J(^{11}B,C^{19}F_3)$	27.1	26.9	27.1	27.0	36 ± 2	25.9
$^2J(^{11}B,C(O)^{19}F)$	51.7					
$^2J(^{17}O,C(O)^{19}F)$	~40					
$^3J(^{13}CF_3,^{12}C^{19}F_3)$	4.0	3.6	3.6	4	n.o.[d]	3.9
$^3J(^{13}CO,^{12}C^{19}F_3)$	4.0	3.9	3.6	n.o.	n.o.	
$^4J(^{12}C^{19}F_3,^{13}C^{19}F_3)$	6.3	6.3	6.3	n.o.	6.1	5.8
$^4J(^{12}C^{19}F_3,C(O)^{19}F)$	7.6					
ref.	[e]	[e]	[e]	[e]	[8][e]	[4]

[a] δ in ppm, J in Hz. [b] NMR solvent: CD_3CN. [c] NMR solvent: CD_2Cl_2. [d] n.o. = not observed. [e] This work.

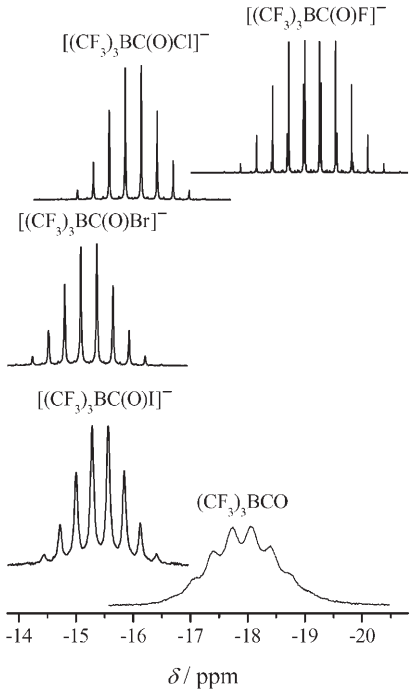

Figure 3. ^{11}B NMR spectra of $(CF_3)_3BCO$ and $[(CF_3)_3BC(O)Hal]^-$ (Hal = F, Cl, Br, I).

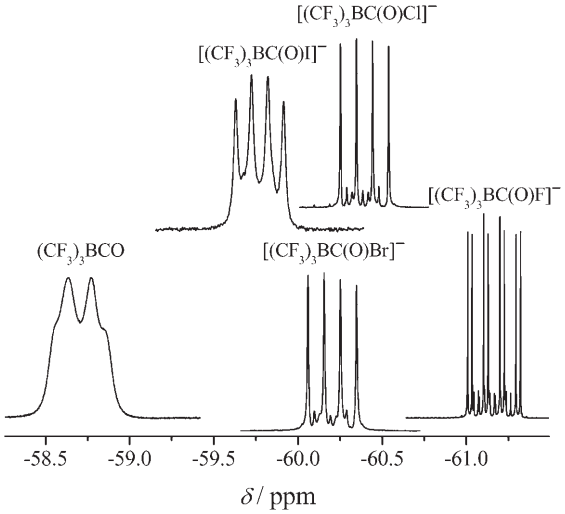

Figure 4. ^{19}F NMR spectra of $(CF_3)_3BCO$ and $[(CF_3)_3BC(O)Hal]^-$ (Hal = F, Cl, Br, I).

coupling.[16] The ^{19}F NMR chemical shift [$\delta(^{19}F) = 78.3$ ppm] and the coupling scheme (quartet of decets; Table 5) of the fluoroacyl substituent have been discussed in detail previously.[16] Similar to the ^{11}B NMR spectra, the line widths of the ^{19}F NMR signals increase from the fluorine derivative to $(CF_3)_3BCO$ as a result of the interaction with the central ^{11}B nucleus. In contrast to ^{11}B NMR spectroscopy the coupling pattern of the ^{19}F NMR signals of $(CF_3)_3BCO$ and $[(CF_3)_3BC(O)I]^-$ are distorted and do not exhibit the correct coupling constants (Figure 4 and Table 5). Both phenomena are explained by quadrupolar relaxation, which is well-known for a nucleus A that couples to a nucleus B with spin $S > 1/2$, and an inverse spin–lattice relaxation rate σ_1 (Table S8 in the Supporting Information) comparable to the coupling constant $^nJ(A,B)$.[8,52–54] Owing to the small line widths of $[(CF_3)_3BC(O)Hal]^-$ (Hal = F, Cl, Br) the ^{10}B satellites are observed (Figure 4 and Table S7 in the Supporting Information).

In the ^{13}C NMR spectra of $[(CF_3)_3BC(O)Hal]^-$ (Hal = F, Cl, Br, I) and $(CF_3)_3BCO$[8] two signals are observed with a relative intensity of 3:1 for the three CF_3 groups and the haloacyl/carbonyl ligands, respectively. The observed trends in the line widths and the distortions of the signals in the ^{13}C NMR spectra are comparable to those observed in the ^{19}F NMR spectra described above. The ^{13}C NMR chemical shifts of the CF_3 groups (Table 5) appear in the region typical for trifluoromethyl groups.[55] All the signals of the CF_3

groups are split into quartets [$^1J(^{13}CF_3,^{13}C^{19}F_3)$] of quartets [$^1J(^{11}B,^{13}CF_3)$] of septets [$^3J(^{13}CF_3,^{12}C^{19}F_3)$] (Table 5). The $^1J(^{11}B,^{13}CF_3)$ coupling constants increase from $[(CF_3)_3BC(O)F]^-$ to $(CF_3)_3BCO$, analogous to the behavior of $^2J(^{11}B,C^{19}F_3)$ (Table 5). This trend also indicates relatively strong B–CF_3 bonds in the borane carbonyl, weaker bonds in the acyl complexes, and even weaker σ bonds in the $[B(CF_3)_4]^-$ ion.

The signals of the ^{13}C nuclei of the haloacyl/carbonyl ligands are found at higher chemical shifts than those of the trifluoromethyl groups. In the isovalent-electronic series $\delta(^{13}C(O))$ increases in the following order: $(CF_3)_3BCO < [(CF_3)_3BC(O)F]^- < [(CF_3)_3BC(O)Cl]^- \sim [(CF_3)_3BC(O)Br]^- < [(CF_3)_3BC(O)I]^-$ (Table 5 and Figure 5). The signals exhibit coupling to ^{11}B (quartet) and to the nine equivalent ^{19}F nuclei of the CF_3 groups (decet). For $[(CF_3)_3BC(O)F]^-$ the interaction with the nucleus of the directly bonded fluorine atom (doublet) is also observed.[16] The coupling constants $^1J(^{11}B,^{13}C(O))$ are plotted against d(C–O) and d(B–C) in Figure 6. As $^1J(^{11}B,^{13}C(O))$ increases the B–C bond lengths shorten and the C–O bond lengths increase.

It was possible to record the ^{17}O NMR spectra of $[(CF_3)_3BC(O)Hal]^-$ (Hal = F, Cl, Br, I) and $(CF_3)_3BCO$ despite the broad lines (20–110 Hz) resulting from the quadrupolar moment of ^{17}O ($eQ = -2.6\times10^{-26}\,e\,cm^2$, $I = 5/2$)[56] and the low natural abundance of ^{17}O (0.037 %).[56] The ^{17}O NMR chemical shift of $(CF_3)_3BCO$ [$\delta(^{17}O) = 342$ ppm] lies between those of neutral transition-metal carbonyls,[56] for example, $Ni(CO)_4$ [$\delta(^{17}O) = 362$ ppm][57] and $MeCO^+$ [$\delta(^{17}O) = 299.5$ ppm].[15] Relative to the related $MeCO^+$/MeC(O)Hal and FC(O)Hal (Hal = F, Cl, Br, I) series, the ^{17}O NMR signals of $[(CF_3)_3BC(O)Hal]^-$ (Hal = F, Cl, Br, I) are shifted to higher frequencies, as shown in Table 6 and Figure 5. Increasing ^{17}O resonance frequencies from iodo- to fluoroacyl derivatives are observed for $[(CF_3)_3BC(O)Hal]^-$ (Hal = F, Cl, Br, I) as well as for FC(O)Hal and MeC(O)Hal (Table 6 and Figure 5). The data for $(CF_3)_3BCO$ and $MeCO^+$[15] fit into this trend whereas no data is available for FCO^+.[66] In contrast to the increase in $\delta(^{17}O)$ a similar trend in $\delta(^{13}C(O))$ is only found for $[(CF_3)_3BC(O)Hal]^-$ (Hal = F, Cl, Br, I) (Figure 5); for $MeCO^+$/MeC(O)Hal and FC(O)Hal (Hal = F, Cl, Br, I), $\delta(^{13}C(O))$ decreases from the

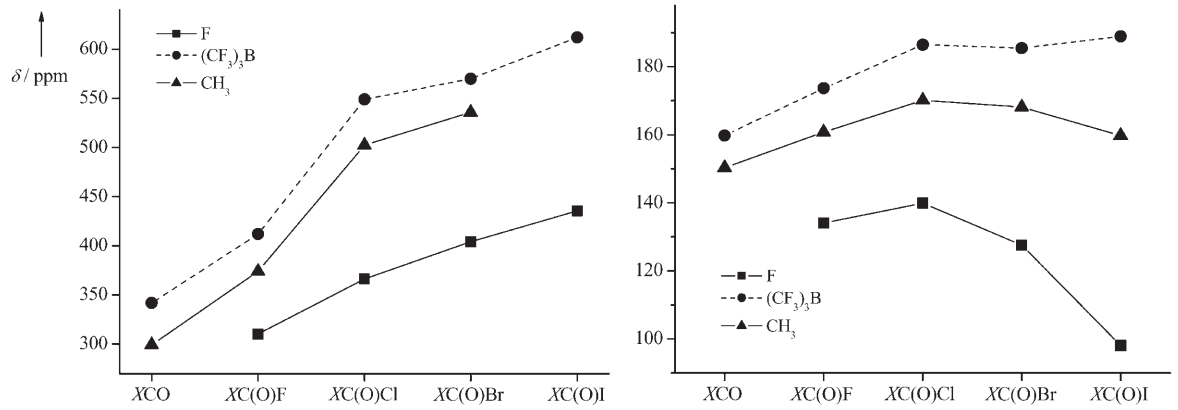

Figure 5. Comparison of ^{17}O (left) and ^{13}C chemical shifts (right) of $[(CF_3)_3BC(O)Hal]^-$, FC(O)Hal, MeC(O)Hal (Hal = F, Cl, Br, I), $(CF_3)_3BCO$, and $MeCO^+$.

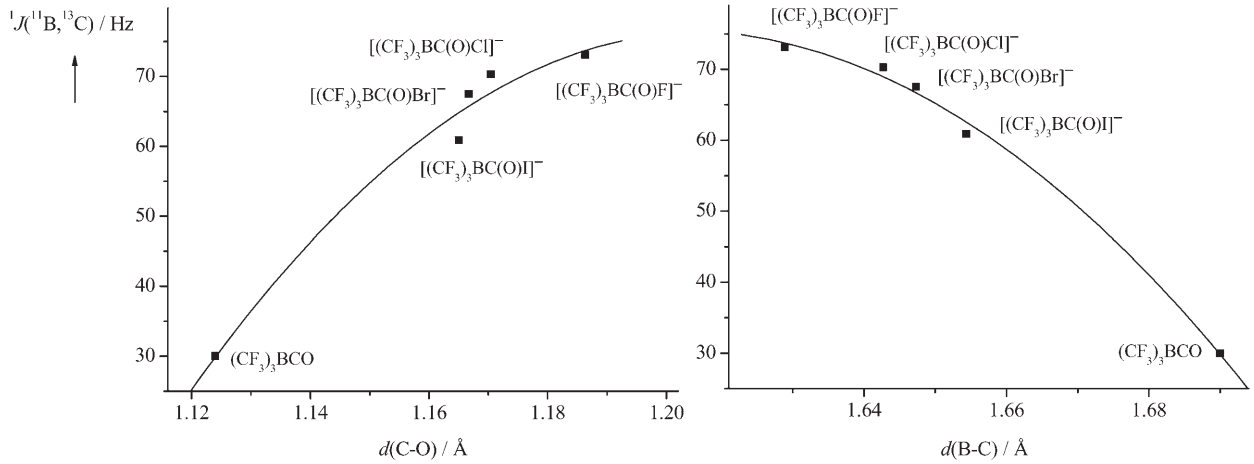

Figure 6. Plot of $^1J(^{11}B,^{13}C(O))$ against d(C–O) (left) and d(B–C(O)) (right) for $(CF_3)_3BCO$ and $[(CF_3)_3BC(O)Hal]^-$ (Hal = F, Cl, Br, I) [d(B–C(O)) and d(C–O) are either experimental or calculated values].

Table 6. ^{13}C and ^{17}O NMR chemical shifts of $[(CF_3)_3BC(O)Hal]^-$, MeC(O)Hal, and FC(O)Hal (Hal = F, Cl, Br, I).

	$\delta(^{13}C)$[a]	$\delta(^{17}O)$[a]	Ref.		$\delta(^{13}C)$[a]	$\delta(^{17}O)$[a]	Ref.		$\delta(^{13}C)$[a]	$\delta(^{17}O)$[a]	Ref.
$(CF_3)_3BCO$	159.8	342	[7,8][b]	CH_3CO^+	150.3	299.5	[15,60]				
$[(CF_3)_3BC(O)F]^-$	173.7	412	[b]	$CH_3C(O)F$	160.8	374	[61,64]	FC(O)F	134.1	310.3	[58]
$[(CF_3)_3BC(O)Cl]^-$	186.5	549	[b]	$CH_3C(O)Cl$	170.1	502.5	[59,62]	FC(O)Cl	139.9	366.4	[58]
$[(CF_3)_3BC(O)Br]^-$	185.5	570	[b]	$CH_3C(O)Br$	168.1	536	[59,65]	FC(O)Br	127.6	404.2	[58]
$[(CF_3)_3BC(O)I]^-$	188.9	612	[b]	$CH_3C(O)I$	159.8	n.o.[c]	[63]	FC(O)I	98.1	435.7	[49]

[a] δ in ppm. [b] This work. [c] n.o. = not observed.

chloro- to the iodoacyl derivative. The differences in the trends of $\delta(^{17}O)$ and $\delta(^{13}C(O))$ are due to the direct bond between the carbonyl carbon atom and the halogen atoms which have no direct influence on the oxygen nuclei. The shorter C(O)–Hal distance in MeC(O)Hal and FC(O)Hal than in $[(CF_3)_3BC(O)Hal]^-$ explains the stronger influence of the halogen atoms on $\delta(^{13}C(O))$ in the first two series.

Owing to the broad lines of the ^{17}O NMR signals no couplings to the nuclei of the $(CF_3)_3B$ fragments in $[(CF_3)_3BC(O)Hal]^-$ (Hal = F, Cl, Br, I) and $(CF_3)_3BCO$ can be observed. The ^{17}O NMR signal of the $[(CF_3)_3BC(O)F]^-$ anion is split into a doublet as a result of ^2J coupling to the ^{19}F nucleus of the fluoroacyl ligand [$^2J(^{17}O,C(O)^{19}F) \sim 40$ Hz]. Similar ^2J coupling constants have been described for other fluoroacyl species, for example, MeC(O)F[64] and FC(O)F.[58]

Vibrational spectra: The IR and Raman spectra of K-$[(CF_3)_3BC(O)F]$ and Cs$[(CF_3)_3BC(O)F]$ have been discussed in detail previously.[16] Herein we present the spectra of the corresponding $[nBu_4N]^+$ salt. The anion bands in the spectra of $[nBu_4N][(CF_3)_3BC(O)F]$ have been assigned by comparison with the spectra of the corresponding K^+ salt. For the three $[(CF_3)_3BC(O)F]^-$ salts, ν(C–O) decreases in the order K^+ (1829 cm^{-1})[16] > Cs^+ (1819 cm^{-1})[16] > [nBu4N]$^+$ (1816 cm^{-1}). This trend is explained by a decrease in the interaction between the cation and the borate anion. The C(O)F···K interaction weakens the C–F bond and strengthens the C=O bond.

Owing to the instability of the haloacylborate anions $[(CF_3)_3BC(O)Hal]^-$ (Hal = Cl, Br, I) in alkali metal salts their IR and Raman spectra could not be obtained. Hence, the vibrational spectra of $[nBu_4N][(CF_3)_3BC(O)Hal]$ (Hal = Cl, Br, I) were investigated, but the anion bands are partially overlapped by cation bands. The cation bands were identified by comparison with the spectra of $[nBu_4N]$-$[(CF_3)_3BC(O)F]$ and $[nBu_4N][B(CN)_4]$[5] and the anion modes by comparison with the spectra predicted by DFT calculations. The experimental and theoretical wavenumbers for the vibrations of the C(O)Hal moiety (Hal = F, Cl, Br, I) are collected in Table 7 and complete Tables of the measured and calculated vibrational data are given in the Supporting Information (Tables S3–S6). The vibrational spectra of $[nBu_4N][(CF_3)_3BC(O)Hal]$ (Hal = F, Cl, Br, I) are depicted in Figure 7.

The band position of the $(CF_3)_3B$ fragments, which range from 1300 to 400 cm^{-1}, are very similar (Figure 7, Tables S3–S6 in the Supporting Information) and are also comparable to the band patterns of other tris(trifluoromethyl)boron derivatives.[2–4,8] The band positions as well as the intensities of the vibrations that can be attributed to the C(O)Hal ligands (Hal = F, Cl, Br, I) are strongly dependent on the halogen (Table 7). The CO stretches are in the range typical of other haloacyl compounds, for example, MeC(O)Hal or FC(O)Hal (Hal = F, Cl, Br, I), as presented in Figure 2. There is no clear trend in the values of ν(CO) in the series $[(CF_3)_3BC(O)Hal]^-$ (Hal = F, Cl, Br, I) as in MeC(O)Hal and FC(O)Hal. The values of ν(C–Hal) decrease from the fluoro- to the iodoacyl complex. The assignment of bands to ν(B–C(O)Hal) is uncertain because strong coupling with ν_s-(B–CF_3) (A′) takes place as indicated by DFT calculations, hence, two values are given in Table 7. While the lower values for ν(B–C(O)Hal)/ν_s(B–C) derived from DFT calculations show a low dependence on the halogen atom, the vibrations with the higher wavenumber decrease from chlorine to iodine. In the case of $[(CF_3)_3BC(O)F]^-$, ν(B–C(O)Hal)/ν_s(B–C) with the higher value is also coupled with ν(C–F) (1077 cm^{-1}) resulting in a lower value (852 cm^{-1}) compared to its higher homologues. As expected the wavenumbers for the deformation modes δ(HalCO) and π(HalCO) decrease from fluorine to iodine.

Table 7. Experimental and calculated[a] band positions of the C(O)Hal fragment in $[(CF_3)_3BC(O)Hal]^-$ (Hal = F, Cl, Br, I).[b]

Assignment[c]		$[(CF_3)_3BC(O)F]^-$[d]			$[(CF_3)_3BC(O)Cl]^-$[e]			$[(CF_3)_3BC(O)Br]^-$[e]			$[(CF_3)_3BC(O)I]^-$[e]		
		Calcd	IR	Ra	Calcd	IR	Ra	Calcd	IR	Ra	Calcd	IR	Ra
ν(CO)	A′	1871	1829	1829	1894	1801	1804	1920	1819	1826	1946	1810	1810
ν(CHal)	A′	1053	1077	n.o.[f]	653	655	661	622	624	631	591	599	608
ν(B–C(O))[g]	A′	838	852	855	954	979	n.o.	933	959	n.o.	913	942	n.o.
	A′	271	289	279	272	n.o.	270	271	n.o.	n.o.	272	n.o.	n.o.
δ(HalCO)	A′	655	667	667	384	n.o.	399	345	n.o.	354	338	n.o.	346
π(HalCO)	A″	600	601	n.o.	506	516	520	496	501	n.o.	483	490	n.o.
ρ(HalCO)	A′	340	354	353	198	n.o.	208	118	n.o.	128	79	n.o.	n.o.

[a] At the B3LYP/6-311+G(d) level of theory. [b] Wavenumbers in cm^{-1}. [c] According to C_s symmetry. [d] K^+ salt, Cs^+: ν(CO) = 1819 cm^{-1}; $[nBu_4N]^+$: 1816 cm^{-1}. [e] $[nBu_4N]^+$ salt. [f] n.o. = not observed. [g] ν(B–C(O)) is strongly mixed with ν(B–CF_3) (A′).

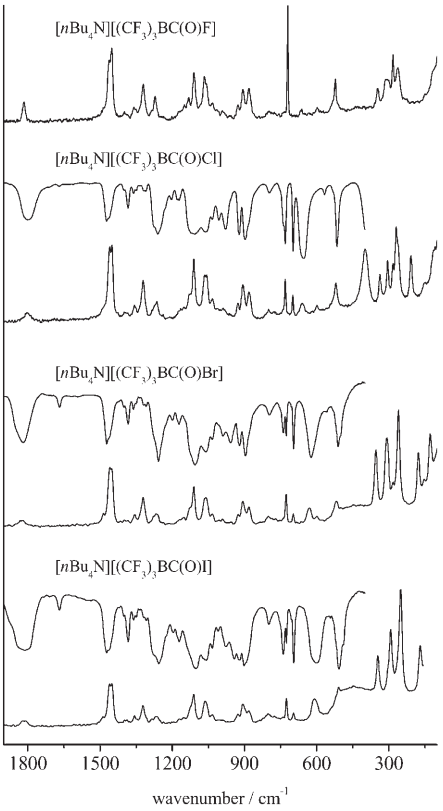

Figure 7. IR and Raman spectra of $[n\mathrm{Bu_4N}][(\mathrm{CF_3})_3\mathrm{BC(O)Hal}]^-$ (Hal = F, Cl, Br, I).

Summary and Conclusions

The synthesis of haloacylborates has been a challenge in mononuclear borane carbonyl chemistry. Their unprecedented high thermal stabilities have enabled detailed spectroscopic as well as structural investigations. A comparison of the properties of the haloacylboron complexes with those of the similar neutral MeC(O)Hal and FC(O)Hal (Hal = F, Cl, Br, I) compounds reveals some substantial differences, for example, elongated C(O)–Hal bonds in the borate anions or different trends in the ^{13}C chemical shifts of the carbonyl carbon atoms. These differences have been attributed to the negative charge of $[(\mathrm{CF_3})_3\mathrm{BC(O)Hal}]^-$ (Hal = F, Cl, Br, I) in comparison to the related neutral species, which also result in lower C(O)–Hal bond energies. To a lesser extent the different properties of the haloacylboron compounds are due to the sterically demanding $(\mathrm{CF_3})_3\mathrm{B}$ group. An example of a trend followed by all three haloacyl series is the decrease in the thermal stability from the fluoroacyl to the corresponding iodoacyl derivative.

A first glance at the chemistry of $[(\mathrm{CF_3})_3\mathrm{BC(O)Hal}]^-$ (Hal = F, Cl) ions has been presented; for example, the syntheses of the first phospha- and arsaethynyl complexes of boron.[16] The different reactivities of $(\mathrm{CF_3})_3\mathrm{BCO}$, $[(\mathrm{CF_3})_3\mathrm{BC(O)F}]^-$, and $[(\mathrm{CF_3})_3\mathrm{BC(O)Cl}]^-$ with the same reagents result in different products. The advantages of $[(\mathrm{CF_3})_3\mathrm{BC(O)Hal}]^-$ (Hal = F, Cl) over the borane carbonyl in synthetic reactions is their solid nature and higher thermal stability, which allows easy storage and handling in a glove box.

Experimental Section

Apparatus: Volatile materials were manipulated in glass vacuum apparatus of known volume equipped with valves with PTFE stems (Young, London) and with capacitance pressure gauges (Type 280E, Setra Instruments, Acton, MA). Solid materials were manipulated inside an inert atmosphere box (Braun, Munich, Germany) filled with argon and with a residual moisture content of less than 0.1 ppm.

Chemicals: All standard chemicals were obtained from commercial sources. Solvents were dried and stored over molecular sieves (4 Å) under nitrogen in flasks equipped with valves with PTFE stems (Young, London). $(\mathrm{CF_3})_3\mathrm{BCO}$ was prepared by the acidic hydrolysis of $K[B(CF_3)_4]$ with H_2SO_4 as reported previously[7,8] and stored in flame-sealed glass ampoules under liquid nitrogen in a Dewar storage vessel. NOCl was obtained from Merck-Schuchardt. $K[(\mathrm{CF_3})_3\mathrm{BC(O)F}]$ was prepared according to the literature procedure.[16] Ampoules were opened and flame-sealed again using an ampoule key.[67]

Vibrational spectroscopy: Infrared spectra were recorded at room temperature with an IFS-66v FT spectrometer (Bruker, Karlsruhe, Germany). For each spectrum 64 scans were co-added with an apodized resolution of 2 cm^{-1}. The samples were measured between AgBr discs or as Nujol mulls between AgBr discs in the region of 4000–400 cm^{-1}. Raman spectra were recorded at room temperature with a Bruker RFS100/S FT Raman spectrometer using the 1064 nm exciting line of a Nd/YAG laser. Crystalline samples in large melting point capillaries (2 mm o.d.) were used to record spectra in the region of 3500–50 cm^{-1} with a resolution of 1 cm^{-1}. For each spectrum 256 scans were co-added and the Raman intensities were corrected by calibration of the spectrometer with a tungsten halogen lamp.

Differential scanning calorimetry: Thermo-analytical measurements were made with a Netzsch DSC204 instrument. Temperature and sensitivity calibrations in the temperature range of 20–500 °C were carried out with naphthalene, benzoic acid, KNO_3, $AgNO_3$, $LiNO_3$, and CsCl. Solid samples (about 5–10 mg) were weighed and placed in sealed aluminium crucibles. They were studied in the temperature range of 20–500 °C at a heating rate of 5 K min^{-1}; throughout this process the furnace was flushed with dry nitrogen. To evaluate the output, the Netzsch Protens4.0 software was employed.

NMR spectroscopy: ^1H, ^{17}O, ^{19}F, and ^{11}B NMR spectra were recorded at room temperature with a Bruker Avance DRX-300 spectrometer operating at 300.13, 40.69, 282.41, and 96.92 MHz for ^1H, ^{17}O, ^{19}F, and ^{11}B nuclei, respectively. ^{13}C NMR spectroscopic studies were performed at room temperature with a Bruker Avance DRX-500 spectrometer operating at 125.758 MHz. The NMR signals were referenced against TMS (^1H and ^{13}C), $CFCl_3$ (^{19}F), $BF_3{\cdot}OEt_2$ in CD_3CN (^{11}B), and H_2O (^{17}O) as external standards. Samples of moisture-sensitive compounds for NMR spectroscopic studies and reactions monitored by NMR spectroscopy were prepared in 5 mm NMR tubes equipped with special valves with PTFE stems (Young, London).[68] Dry CD_2Cl_2 or CD_3CN was used as the solvent.

Single-crystal X-ray diffraction: Crystals of $[PPh_4][(\mathrm{CF_3})_3\mathrm{BC(O)Br}]$ suitable for X-ray diffraction were obtained from CH_2Cl_2 solution by slow uptake of pentane vapor. Diffraction data were collected at 100 K with a KappaCCD diffractometer (Bruker AXS) using $Mo_{K\alpha}$ radiation (λ = 0.71073 Å) and a graphite monochromator. The crystal structure was determined by using SHELXS-97[69] and full-matrix least-squares refinement based on F^2 was performed using SHELXL-97.[70] Integration and empirical absorption corrections (DENZO scalepack)[71] were applied. Molecular structure diagrams were drawn by using the Diamond program.[72] The experimental details and crystal data are summarized in Table 3.

Quantum-chemical calculations: DFT calculations[73] were carried out using Becke's three-parameter hybrid functional and the Lee–Yang–Parr correlation functional (B3LYP)[74–76] with the Gaussian 98 suite of programs.[77] Geometries were optimized and energies calculated with the 6-311++G(d) basis set and all structures represent true minima on the respective hypersurface (no imaginary frequency). Diffuse functions were incorporated because improved energies are obtained for anions.[78] All energies presented herein are zero-point corrected and thermal contributions are included in enthalpies and free energies calculated for 298 K.

Synthetic reactions

[*n*Bu$_4$N][(CF$_3$)$_3$BC(O)F]: A 50 mL round-bottom flask equipped with a valve with a PTFE stem (Young, London), fitted with a PTFE-coated magnetic stirring bar, and placed inside a dry box was charged with K-[(CF$_3$)$_3$BC(O)F] (579 mg, 1.9 mmol) and [*n*Bu$_4$N]Cl (476 mg, 1.7 mmol). The reaction vessel was attached to a glass vacuum apparatus and CH_2Cl_2 (40 mL) was added under nitrogen. The reaction mixture was stirred for 2 h. The resulting suspension was filtered through a Schlenk frit charged with Celite. The residue and the frit were washed with CH_2Cl_2 (40 mL). All volatiles were removed under vacuum and a colorless solid was obtained. Yield based on [*n*Bu$_4$N]Cl: 761 mg (1.5 mmol, 90%); elemental analysis calcd (%) for $C_{18}H_{36}BF_{10}NO$: C 47.35, H 7.15, N 2.76; found: C 46.75, H 7.50, N 2.78.

[*n*Bu$_4$N][(CF$_3$)$_3$BC(O)Cl]: Inside a dry box [*n*Bu$_4$N]Cl (1.06 g, 3.8 mmol) was placed in a 100 mL round-bottom flask equipped with a valve with a PTFE stem (Young, London) and fitted with a PTFE-coated magnetic stirring bar. At −196 °C (CF$_3$)$_3$BCO (990 mg, 4.0 mmol) followed by dichloromethane (25 mL) were transferred to the vessel under vacuum. The flask was placed in a cold bath at −80 °C and while stirring the reaction mixture was allowed to warm to room temperature overnight. All volatiles were removed in vacuo to yield a colorless solid. Yield based on [*n*Bu$_4$N]Cl: 1.94 g (3.7 mmol, 97%); purity determined by ^{19}F NMR spectroscopy: 98%; elemental analysis calcd (%) for $C_{20}H_{36}BClF_9NO$: C 45.86, N 2.67; found: C 45.72, N 2.75.

[Et$_4$N][(CF$_3$)$_3$BC(O)Cl], [Ph$_4$P][(CF$_3$)$_3$BC(O)Cl], [*n*Bu$_4$N][(CF$_3$)$_3$BC(O)Br], [Ph$_4$P][(CF$_3$)$_3$BC(O)Br], and [*n*Bu$_4$N][(CF$_3$)$_3$BC(O)I]: The title salts were synthesized according to the procedure described for the preparation of [*n*Bu$_4$N][(CF$_3$)$_3$BC(O)Cl] using (CF$_3$)$_3$BCO and [Et$_4$N]Cl, [Ph$_4$P]Cl, [*n*Bu$_4$N]Br, [Ph$_4$P]Br, or [*n*Bu$_4$N]I as the starting materials.

[Et$_4$N][(CF$_3$)$_3$BC(O)Cl]: Yield based on [Et$_4$N]Cl: 1.07 g (2.6 mmol, 96%); purity determined by ^{19}F NMR spectroscopy: 98%; elemental analysis calcd (%) for $C_{12}H_{20}BClF_9NO$: C 35.02, H 4.90, N 3.40; found: C 35.64, H 5.09, N 3.41.

[Ph$_4$P][(CF$_3$)$_3$BC(O)Cl]: Yield based on [Ph$_4$P]Cl: 1.68 mg (2.7 mmol, 96%); purity determined by ^{19}F NMR spectroscopy: 98%; elemental analysis calcd (%) for $C_{28}H_{20}BClF_9OP$: C 54.18, H 3.25; found: C 54.80, H 3.24.

[*n*Bu$_4$N][(CF$_3$)$_3$BC(O)Br]: Yield based on [*n*Bu$_4$N]Br: 1.70 g (3.0 mmol, 97%); purity determined by ^{19}F NMR spectroscopy: 98%; elemental analysis calcd (%) for $C_{20}H_{36}BBrF_9NO$: C 42.28, N 2.47; found: C 42.03, N 2.56.

[Ph$_4$P][(CF$_3$)$_3$BC(O)Br]: Yield based on [Ph$_4$P]Br: 665 mg (1.0 mmol, 98%); purity determined by ^{19}F NMR spectroscopy: 98%; elemental analysis calcd (%) for $C_{28}H_{20}BBrF_9OP$: C 50.56, H 3.03; found: C 51.04, H 3.01.

[*n*Bu$_4$N][(CF$_3$)$_3$BC(O)I]—Method A: Yield based on [*n*Bu$_4$N]I: 492 mg (0.8 mmol, 95%); purity determined by ^{19}F NMR spectroscopy: 98%; elemental analysis calcd (%) for $C_{20}H_{36}BF_9INO$: C 39.05, N 2.28; found: C 40.07, N 2.29.

[*n*Bu$_4$N][(CF$_3$)$_3$BC(O)I]—Method B: [*n*Bu$_4$N][(CF$_3$)$_3$BC(O)F] (146 mg, 0.29 mmol) was weighed into a 15 mL glass tube equipped with a valve with a PTFE stem (Young, London), fitted with a PTFE-coated magnetic stirring bar, and placed inside a dry box. Dichloromethane (5 mL) and Me_3SiI (0.5 mL, 1.8 mmol) were added by syringe under nitrogen. The colorless solution was stirred overnight. After removal of all volatiles under vacuum a colorless solid was obtained. Yield: 177 mg (0.29 mmol, 99%).

Reaction of (CF$_3$)$_3$BCO with [Et$_3$NH]Cl in CD_2Cl_2: A 5 mm o.d. NMR tube equipped with a valve with a PTFE stem (Young, London)[68] was charged with [Et$_3$NH]Cl (56 mg, 0.41 mmol). (CF$_3$)$_3$BCO (75 mg, 0.31 mmol) and CD_2Cl_2 (1 mL) were added under vacuum at −196 °C. The reaction mixture was warmed to room temperature and analyzed by NMR spectroscopy: 86% [Et$_3$NH][(CF$_3$)$_3$BC(O)Cl], 10% [Et$_3$NH]-[(CF$_3$)$_3$BCl], and 4% other perfluoroalkylborate salts.

The reaction mixture was kept for 18 h at room temperature and then NMR spectra were recorded again: 60% [Et$_3$NH][(CF$_3$)$_3$BC(O)Cl], 30% [Et$_3$NH][(CF$_3$)$_3$BCl] and 10% other perfluoroalkylborate salts.

Reaction of (CF$_3$)$_3$BCO with HCl in Et$_2$O: (CF$_3$)$_3$BCO (75 mg, 0.31 mmol) and Et_2O (1 mL) were transferred under vacuum to a 5 mm o.d. NMR tube equipped with a valve with a PTFE stem (Young, London).[68] A 50 mL flask equipped with a valve with a PTFE stem (Young, London) was charged with HCl (0.9 mmol). The flask was connected to the NMR tube and the HCl was allowed to diffuse into the borane carbonyl solution which was kept at −100 °C. Within 30 minutes a colorless solid had precipitated from the solution. All volatiles were then removed at −100 °C under reduced pressure. CD_2Cl_2 (1 mL) was condensed into the NMR tube at −196 °C. The solution was warmed to −50 °C, and NMR spectra were recorded: analysis of the spectra revealed the formation of [H(OEt$_2$)$_2$][(CF$_3$)$_3$BC(O)Cl]. ^{1}H NMR data for the [H-(OEt$_2$)$_2$]$^+$ cation: δ = 16.3 (s, O-H$^+$-O), 4.1 (q, 8H, $^1J_{H,C}$ = 150.0 Hz, $^3J_{H,H}$ = 7.2 Hz, $^1\Delta H(^{12,13}C)$ = 0.0034 ppm, CH_2), 1.4 ppm (t, 12H, $^1J_{H,C}$ = 128.4 Hz, $^3J_{H,H}$ = 7.2 Hz, $^1\Delta H(^{12,13}C)$ = 0.0030 ppm, CH_3).

The reaction mixture was then warmed to room temperature. After 14 h an orange solution was obtained. Complex NMR spectra were obtained and hence a complete assignment was impossible although [(CF$_3$)$_3$BCl]$^-$[30] and [(CF$_3$)$_3$BF]$^-$,[30,31] which were formed in small quantities, were identified.

NO[(CF$_3$)$_3$BCl]: At −196 °C (CF$_3$)$_3$BCO (840 mg, 3.4 mmol) and NOCl (5 mL) were condensed into 100 mL round-bottom flask equipped with a valve with a PTFE stem (Young, London) and fitted with a PTFE-coated magnetic stirring bar. After warming to room temperature a clear colorless solution was obtained that was stirred overnight. All volatiles were removed in vacuo and a colorless solid was obtained. The residue was analyzed by ^{11}B and ^{19}F NMR spectroscopy: 79% NO[(CF$_3$)$_3$BCl], 13% NO[(CF$_3$)$_3$BF], 1% NO[$C_2F_5BF_3$], and 7% unidentified products. NMR data of the [(CF$_3$)$_3$BCl]$^-$ ion: ^{19}F NMR: δ = −65.8 ppm (q, $^1J_{C,F}$ = 303.5 Hz, $^2J_{B,F}$ ≈ 30 Hz, $^4J_{F,F}$ = 6.1 Hz, $^1\Delta F(^{12,13}C)$ = 0.1303 ppm, $^3\Delta F(^{35,37}Cl)$ = 0.0014 ppm); ^{11}B NMR: δ = −12.7 ppm (decet, $^1J_{B,C}$ ≈ 82 Hz, $^2J_{B,F}$ = 30.2 Hz, $^1\Delta B(^{12,13}C)$ = 0.0005 ppm).[30]

Acknowledgements

Financial support by the Deutsche Forschungsgemeinschaft (DFG) is acknowledged. Furthermore, we are grateful to Merck KGaA (Darmstadt, Germany) for providing additional financial support and chemicals used in this study.

[1] G. Pawelke, *J. Fluorine Chem.* **1989**, *42*, 429.
[2] G. Pawelke, H. Bürger, *Coord. Chem. Rev.* **2001**, *215*, 243.
[3] G. Pawelke, H. Bürger, *Appl. Organomet. Chem.* **1996**, *10*, 147.
[4] E. Bernhardt, G. Henkel, H. Willner, G. Pawelke, H. Bürger, *Chem. Eur. J.* **2001**, *7*, 4696.
[5] E. Bernhardt, G. Henkel, H. Willner, *Z. Anorg. Allg. Chem.* **2000**, *626*, 560.
[6] E. Bernhardt, M. Finze, H. Willner, *Z. Anorg. Allg. Chem.* **2003**, *629*, 1229.
[7] A. Terheiden, E. Bernhardt, H. Willner, F. Aubke, *Angew. Chem.* **2002**, *114*, 823; *Angew. Chem. Int. Ed.* **2002**, *41*, 799.
[8] M. Finze, E. Bernhardt, A. Terheiden, M. Berkei, H. Willner, D. Christen, H. Oberhammer, F. Aubke, *J. Am. Chem. Soc.* **2002**, *124*, 15385.

[9] H. Willner, F. Aubke, *Organometallics* **2003**, *22*, 3612.
[10] H. Willner, F. Aubke, *Chem. Eur. J.* **2003**, *9*, 1668.
[11] H. Willner, F. Aubke in *Inorganic Chemistry Highlights, Vol. 2* (Eds.: G. Meyer, L. Wesemann, D. Naumann), Wiley-VCH, Weinheim, **2002**, p. 195.
[12] H. Willner, F. Aubke, *Angew. Chem.* **1997**, *109*, 2506; *Angew. Chem. Int. Ed. Engl.* **1997**, *36*, 2402.
[13] C. Bach, H. Willner, C. Wang, S. J. Rettig, J. Trotter, F. Aubke, *Angew. Chem.* **1996**, *108*, 2104; *Angew. Chem. Int. Ed. Engl.* **1996**, *35*, 1974.
[14] B. von Ahsen, M. Berkei, G. Henkel, H. Willner, F. Aubke, *J. Am. Chem. Soc.* **2002**, *124*, 8371.
[15] G. A. Olah, A. L. Berrier, G. K. S. Prakash, *J. Am. Chem. Soc.* **1982**, *104*, 2373.
[16] M. Finze, E. Bernhardt, H. Willner, C. W. Lehmann, *Angew. Chem.* **2003**, *115*, 1082; *Angew. Chem. Int. Ed.* **2003**, *42*, 1052.
[17] M. Finze, E. Bernhardt, H. Willner, C. W. Lehmann, *Angew. Chem.* **2004**, *116*, 4253; *Angew. Chem. Int. Ed.* **2004**, *43*, 4159.
[18] M. Finze, E. Bernhardt, C. W. Lehmann, H. Willner, *J. Am. Chem. Soc.* **2005**, *127*, in press.
[19] D. F. Burow, *Inorg. Chem.* **1972**, *11*, 573.
[20] W. Eisfeld, M. Regitz, *J. Am. Chem. Soc.* **1996**, *118*, 11918.
[21] A. Kivinen in *The Chemistry of Acyl Halides* (Ed.: S. Patai), Wiley-Interscience, New York, **1972**, p. 177.
[22] A. Ansorge, D. J. Brauer, H. Bürger, B. Krumm, G. Pawelke, *J. Organomet. Chem.* **1993**, *446*, 25.
[23] B. F. Spielvogel, A. T. McPhail, J. A. Knight, C. G. Moreland, C. L. Gatchell, K. W. Morse, *Polyhedron* **1983**, *2*, 1345.
[24] L. I. Zakharkin, V. N. Kalinin, V. V. Gedymin, *Tetrahedron* **1971**, *27*, 1317.
[25] V. F. Mironov, S. Y. Pechurina, V. I. Grigos, *Dokl. Akad. Nauk SSSR* **1976**, *230*, 865.
[26] L. I. Zakharkin, V. A. Ol'shevskaya, N. B. Boiko, *Russ. Chem. Bull.* **1996**, *105*, 680.
[27] A. J. Blake, R. W. Cockman, E. A. V. Ebsworth, J. H. Holloway, *J. Chem. Soc. Chem. Commun.* **1988**, 529.
[28] S. A. Brewer, K. S. Coleman, J. Fawcett, J. H. Holloway, E. G. Hope, D. R. Russel, P. G. Watson, *J. Chem. Soc. Dalton Trans.* **1995**, 1073.
[29] N. E. Kolobova, Z. P. Valueva, E. I. Kazimirchuk, *Izv. Akad. Nauk SSSR Ser. Khim.* **1987**, 1671.
[30] D. J. Brauer, H. Bürger, Y. Chebude, G. Pawelke, *Inorg. Chem.* **1999**, *38*, 3972.
[31] M. Finze, E. Bernhardt, M. Zähres, H. Willner, *Inorg. Chem.* **2004**, *43*, 490.
[32] P. Jutzi, C. Müller, A. Stammler, H.-G. Stammler, *Organometallics* **2000**, *19*, 1442.
[33] A. H. Schmidt, M. Russ, D. Grosse, *Synthesis* **1981**, 216.
[34] R. Sustmann in *Heteroatom Manipulation, Vol. 6* (Eds.: B. M. Trost, I. Fleming, E. Winterfeldt), Pergamon Press, Oxford, **1991**, p. 301.
[35] M. Finze, E. Bernhardt, H. Willner, C. W. Lehmann, *Inorg. Chem.* submitted.
[36] M. B. Smith, J. March, *March's Advanced Organic Chemistry: Reactions, Mechanisms and Structure*, 5th ed., John Wiley & Sons, New York, **2001**.
[37] R. D. Shannon, *Acta Crystallogr.* A, **1976**, *32*, 751.
[38] G. A. Olah, S. J. Kuhn, W. S. Tolgyesi, E. B. Baker, *J. Am. Chem. Soc.* **1962**, *84*, 2733.
[39] F. P. Boer, *J. Am. Chem. Soc.* **1966**, *88*, 1572.
[40] S. Tsuchiya, *J. Mol. Struct.* **1974**, *22*, 77.
[41] J. A. Ramsey, J. A. Ladd, *J. Chem. Soc. B* **1968**, 118.
[42] S. Tsuchiya, M. Kimura, *Bull. Chem. Soc. Jpn.* **1972**, *45*, 736.
[43] S. Tsuchiya, T. Ijima, *J. Mol. Struct.* **1972**, *13*, 327.
[44] M. Nakata, K. Kohata, T. Fukuyama, K. Kuchitzu, C. J. Wilkins, *J. Mol. Struct.* **1980**, *68*, 271.
[45] A. H. Nielsen, T. G. Burke, P. J. H. Woltz, E. A. Jones, *J. Chem. Phys.* **1952**, *20*, 596.
[46] H. Oberhammer, *J. Mol. Struct.* **1980**, *73*, 4310.
[47] G. A. Argüello, H. Willner, H. Oberhammer, unpublished results.
[48] R. R. Patty, R. T. Lagemann, *Spectrochim. Acta Part A* **1959**, *15*, 60.
[49] M. S. Chiappero, G. A. Argüello, P. Garcia, H. Pernice, H. Willner, H. Oberhammer, K. A. Peterson, J. S. Francisco, *Chem. Eur. J.* **2004**, *10*, 917.
[50] W. Gombler, *J. Am. Chem. Soc.* **1982**, *104*, 6616.
[51] P. S. Hubbard, *J. Chem. Phys.* **1970**, *53*, 985.
[52] T. K. Halstead, P. A. Osment, B. C. Sanctuary, J. Tagenfeldt, I. J. Lowe, *J. Magn. Reson.* **1986**, *67*, 267.
[53] B. Wrackmeyer in *Annual Reports in NMR Spectroscopy, Vol. 20* (Ed.: G. A. Webb), Academic Press, London, **1988**, p. 61.
[54] A. Abragam, *Principles of Nuclear Magnetism*, Clarendon Press, Oxford, **1986**.
[55] H.-O. Kalinowski, S. Berger, S. Braun, *^{13}C NMR-Spektroskopie*, Thieme, Stuttgart, **1984**.
[56] H. C. E. McFarlane, W. McFarlane in *Multinuclear NMR* (Ed.: J. Mason), Plenum Press, New York, **1987**, p. 403.
[57] R. Bramley, B. N. Figges, R. S. Nyholm, *Trans. Faraday Soc.* **1962**, *58*, 1393.
[58] M. J. Parkington, T. A. Ryan, K. R. Seddon, *J. Chem. Soc., Dalton Trans.* **1997**, 251.
[59] H. A. Christ, P. Diehl, H. Schneider, H. Dahn, *Helv. Chim. Acta* **1961**, *98–99*, 55.
[60] G. A. Olah, A. M. White, *J. Am. Chem. Soc.* **1969**, *91*, 5801.
[61] J. Reuben, S. Brownstein, *J. Mol. Spectrosc.* **1967**, *23*, 96.
[62] C. Delseth, T. T. T. Nguyên, J. P. Kintzinger, *Helv. Chim. Acta* **1980**, *63*, 498.
[63] H. M. R. Hoffmann, K. Haase, *Synthesis* **1981**, 715.
[64] R. Wagner, B. Wiedel, W. Günther, H. Görls, E. Anders, *Eur. J. Org. Chem.* **1999**, 2383.
[65] G. B. Savitsky, R. M. Pearson, K. Namikawa, *J. Phys. Chem.* **1965**, *69*, 1425.
[66] K. O. Christe, B. Hoge, J. A. Boatz, G. K. S. Prakash, G. A. Olah, J. A. Sheehy, *Inorg. Chem.* **1999**, *38*, 3132.
[67] W. Gombler, H. Willner, *J. Phys. E* **1987**, *20*, 1286.
[68] W. Gombler, H. Willner, *Int. Lab.* **1984**, 84.
[69] G. M. Sheldrick, SHELXS-97, University of Göttingen (Germany), **1997**.
[70] G. M. Sheldrick, SHELXL-97, University of Göttingen (Germany), **1997**.
[71] Z. Otwinowski, W. Minor, *Methods Enzymol.* **1997**, *276*, 307.
[72] Crystal Impact GbR, Diamond - Visual Crystal Structure Information System, Ver. 2.1, **1996–1999**.
[73] W. Kohn, L. J. Sham, *Phys. Rev. A* **1965**, *140*, 1133.
[74] A. D. Becke, *Phys. Rev. B* **1988**, *38*, 3098.
[75] A. D. Becke, *J. Chem. Phys.* **1993**, *98*, 5648.
[76] C. Lee, W. Yang, R. G. Parr, *Phys. Rev. B* **1988**, *41*, 785.
[77] M. J. Frisch, G. W. Trucks, H. B. Schlegel, G. E. Scuseria, M. A. Robb, J. R. Cheeseman, V. G. Zakrzewski, J. A. Montgomery, R. E. Stratmann, J. C. Burant, S. Dapprich, J. M. Millam, A. D. Daniels, K. N. Kudin, M. C. Strain, O. Farkas, J. Tomasi, V. Barone, M. Cossi, R. Cammi, B. Mennucci, C. Pomelli, C. Adamo, S. Clifford, J. Ochterski, G. A. Petersson, P. Y. Ayala, Q. Cui, K. Morokuma, D. K. Malick, A. D. Rabuck, K. Raghavachari, J. B. Foresman, J. Cioslowski, J. V. Ortiz, B. B. Stefanov, G. Liu, A. Liashenko, P. Piskorz, I. Komaromi, R. Gomperts, R. L. Martin, D. J. Fox, T. Keith, M. A. Al-Laham, C. Y. Peng, A. Nanayakkara, C. Gonzales, M. Challacombe, P. M. W. Gill, B. Johnson, W. Chen, M. W. Wong, J. L. Andres, C. Gonzales, M. Head-Gordon, E. S. Replogle, J. A. Pople, Gaussian 98 (Revision A.6), Gaussian, Inc. Pittsburgh PA, **1998**.
[78] J. C. Rienstra-Kiracofe, G. S. Tschumper, H. F. Schaefer III, S. Nandi, G. B. Ellison, *Chem. Rev.* **2002**, *102*, 231.

Received: January 13, 2005
Revised: April 26, 2005
Published online: August 30, 2005

